Spectroscopic signatures of molecular orbitals in transition metal oxides with a honeycomb lattice

Z. V. Pchelkina, S. V. Streltsov, and I. I. Mazin

Spectroscopic signatures of molecular orbitals in transition metal oxides with a honeycomb lattice.

Z.V. Pchelkina,[1,2,*] S. V. Streltsov,[1,2] and I. I. Mazin[3]

[1] *M.N. Miheev Institute of Metal Physics of Ural Branch of Russian Academy of Sciences, 620137, Ekaterinburg, Russia*
[2] *Theoretical Physics and Applied Mathematics Department,*
Ural Federal University, Mira St. 19, 620002 Ekaterinburg, Russia
[3] *Code 6393, Naval Research Laboratory, Washington, DC 20375, USA*
(Dated: October 31, 2016)

A tendency to form benzene-like molecular orbitals has been recently shown to be a common feature of the $4d$ and $5d$ transition metal oxides with a honeycomb lattice. This tendency competes with other interactions such as the spin-orbit coupling and Hubbard correlations, and can be partially or completely suppressed. In the calculations, $SrRu_2O_6$ presents the cleanest, so far, case of well-formed molecular orbitals, however, direct experimental evidence for or against this proposition has been missing. In this paper, we show that combined photoemission and optical studies can be used to identify molecular orbitals in $SrRu_2O_6$. Symmetry-driven elelction selection rules suppress optical transitions between certain molecular orbitals, while photoemission and inverse photoemission measurements are insensitive to them. Comparing the photoemission and optical conductivity spectra one should be able to observe clear signatures of molecular orbitals.

PACS numbers:

I. INTRODUCTION

Low dimensional ruthenates with a honeycomb lattice have been attracting a lot of attention in recent years. $\alpha-RuCl_3$, which has one hole in the t_{2g} manifold, shows hallmarks of Kitaev physics [1, 2], Li_2RuO_3 with two t_{2g} holes dimerizes in the low-temperature phase [3, 4] and exhibits a valence bond liquid behavior at high temperatures [5, 6], while $SrRu_2O_6$ with a half-filled t_{2g} band shows rather unusual magnetic properties [7]. It has been argued [8] that the physics of these compounds is underscored by competition between the spin-orbit coupling and Hubbard correlations, on one side, direct Ru-Ru one-electron hopping, on the other side, and O-assisted indirect hopping that leads to formation of molecular orbitals (MO), on the third side [9]. *Ab initio* calculations show that MOs appear to dominate in the last compound [8]. In the first two they are mostly suppressed, but at least in $\alpha-RuCl_3$ (and in a similar compound, Na_2IrO_3) they manifest themselves *via* an anomalously large third-neighbor coupling [10].

MOs inevitably occur if transition metals with active t_{2g} orbitals form a honeycomb lattice and t_{2g} electrons can only hop via oxygen p orbitals [11]. In this case, the electronic structure problem maps onto that of the benzene molecule, essentially, a 6-member ring with nearest and next-nearest neighbor hoppings only (t'_1 and t'_2, respectively). The electronic structure then consist of four levels, A_{1g}, E_{1u}, E_{2g}, B_{1u} (E_{1u} and E_{2g} are doubly degenerate), formed by six molecular orbitals. Their energies are: $E_{A_{1g}} = 2(t'_1 + t'_2)$, $E_{E_{1u}} = (t'_1 - t'_2)$, $E_{E_{2g}} = -(t'_1 + t'_2)$, and $E_{B_{1u}} = -2(t'_1 - t'_2)$ [12]. In this approximation, an electron occupying one of the MOs remains fully localized within one of the Ru hexagons, in spite of the fact that the lattice itself is uniform without any dimerization or clusterization [13]. A sketch of the crystal structure of $SrRu_2O_6$ is shown in Fig. 1.

In real materials $t'_1/3 \sim -t'_2 > 0$ and the two highest MO levels, A_{1g} and E_{1u}, turn out to be nearly degenerate [8, 13]. This is conducive for the spin-orbit coupling (SOC) and is the reason why the SOC is so efficient in the case of one t_{2g} hole as in $\alpha-RuCl_3$ or in Na_2IrO_3. Moreover, for the whole range between the weak and the strong SOC limit the highest energy state ($j_{eff} = 1/2$ or A_{1g} in the respective limits) is half-filled and therefore Hubbard correlations are important.

Increasing number of holes, i.e. going from Ru^{3+} to Ru^{4+} makes E_{1u} band half-filled. One may lift the degeneracy and gain some energy not due to the SOC or formation of molecular orbitals on hexagons, but dimerizing lattice (if the elastic energy penalty would not be too large). In this case the system gains considerable covalent energy due to direct $d-d$ hopping (which may be large in the common edge geometry)[14, 15] and forms spin-singlet dimers. This scenario is realized in Li_2RuO_3 [3, 5, 16].

In the case of three t_{2g} holes, Ru^{5+}, we arrive at the situation, when A_{1g} and E_{1u} states are completely empty and the MOs with their large gap between the E_{1u} and E_{2g} states are energetically favorable. In the ionic approximation the energy gain is of the order of $E_{E_{1u}} - E_{E_{2g}} \approx 2t'_1$. Interestingly, the long range Neél antiferromagnetic (AFM) order does not destroy MOs, but even increases this energy gain [8]. These are the reasons why the MOs are so clearly seen in the band structure calculations in $SrRu_2O_6$ [8].

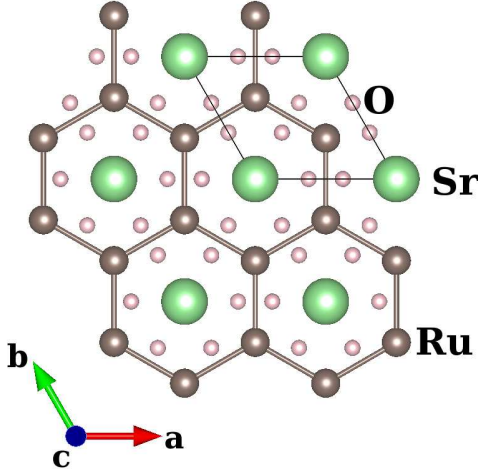While MO scenario has been very successful in explaining the physical properties of $SrRu_2O_6$ [8], no direct ob-

Figure 1: The projection of crystal structure of $SrRu_2O_6$ onto the ab plane. The black line indicates the unit cell boundary.

servation of MOs has been effected so far, and other, albeit, in our opinion, less convincing, scenarios have been proposed [17]. In this paper we suggest that a combination of the spectroscopic techniques sensitive and insensitive to the dipole selection rules may provide direct evidence of the formation of MOs in $SrRu_2O_6$. These can be, *e.g.*, optical absorption and photoemission measurements (the latter are mostly determined by the electronic density of states, DOS), properly corrected for corresponding cross sections. We will show both analytically and numerically that the optical conductivity in the MO picture is dramatically different from the joint DOS, because of unusually restrictive optical selection rules.

II. OPTICAL PROPERTIES OF MOLECULAR ORBITALS

The dipole selection rules prohibit optical transitions between states of the same parity. In the MO picture, this leaves four transitions: $B_{1u} \to E_{2g}$ (at $\hbar\omega = t_1' - 3t_2'$), $E_{2g} \to E_{1u}$ (at $2t_1'$), $E_{1u} \to A_{1g}$ (at $t_1' + 3t_2'$), and $B_{1u} \to A_{1g}$ (at $4t_1'$). For the half filling, representative of $SrRu_2O_6$, that would generate two absorption peaks, corresponding to the $E_{2g} \to E_{1u}$ and $B_{1u} \to A_{1g}$ transitions, the latter at a twice larger energy than the former. However, there is an additional symmetry in the problem that forbids some of these transitions. Indeed, to assure a nonzero optical matrix element, the direct product of the representations of the initial and final states must contain a representation of the corresponding component of the dipole operator p^α (see, *e.g.*, Ref. [18]). In the case of an ideal hexagon with the point group symmetry D_{6h} the p^x and p^y components are transformed according to
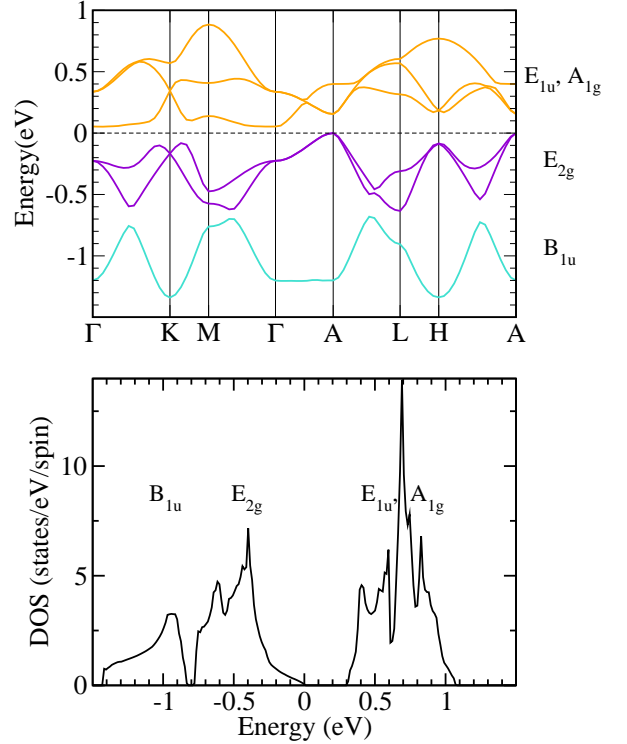

Figure 2: The nonmagnetic GGA band structure (upper panel) and total DOS obtained by GGA calculation for the Néel antiferromagnetic structure (lower panel). The contributions from different molecular orbitals are labeled according to Refs. [8, 12].

the E_{1u} representation [19]. Since

$$B_{1u} \times A_{1g} = B_{1u} \tag{1}$$
$$B_{1u} \times E_{2g} = E_{1u} \tag{2}$$
$$E_{2g} \times E_{1u} = B_{1u} + B_{2u} + E_{1u} \tag{3}$$
$$E_{1u} \times A_{1g} = E_{1u} \tag{4}$$

the point symmetry will suppress $B_{1u} \to A_{1g}$, but not $B_{1u} \to E_{2g}$, $E_{2g} \to E_{1u}$, and $E_{1u} \to A_{1g}$ transitions. In $SrRu_2O_6$ only $E_{2g} \to E_{1u}$ transitions are allowed, but in other hexagonal systems with different number of d electrons one may also expect $B_{1u} \to E_{2g}$ and $E_{1u} \to A_{1g}$ transitions. In Sec. IV we show explicitly the matrix elements of p^α in the nearest- and next-nearest neighbor tight binding approximation. The out-of plane matrix element is zero and corresponding optical transitions are absent in the MO approximation.

Together with the selection rules forbidding transitions between states with the same parity this additional selectivity offers a direct test of the MO scenario. It suggests that despite the double-hump structure of the DOS (Fig. 2), and, correspondingly, joint DOS, the optical absorption $\sigma(\omega)$ will have a one peak structure. Impor-
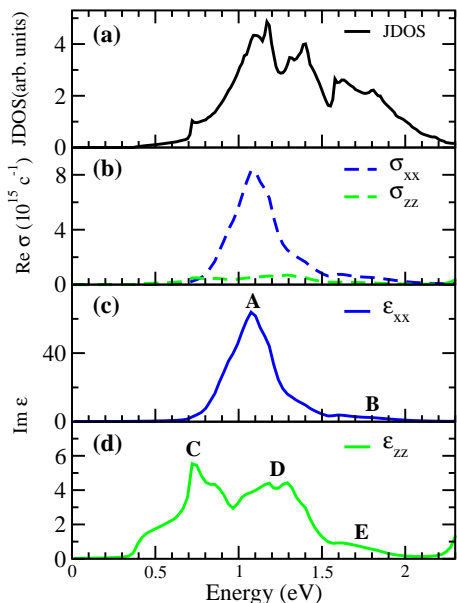
Figure 3: Results of the antiferromagnetic GGA calculations. (a) The joint density of states, $J(\omega)$, is shown by black line. (b) The real part of optical conductivity, Re $\sigma_{\alpha\beta}(\omega) = \frac{\omega}{4\pi} \text{Im } \varepsilon_{\alpha\beta}(\omega)$, where $\alpha, \beta = x$ (blue dotted line) and $\alpha, \beta = z$ (green dotted line). The imaginary part of the frequency-dependent dielectric functions, ε_{xx} (c) and ε_{zz} (d) are shown by solid blue and green lines, correspondingly.

tantly, this is a qualitative, not quantitative test. While the exact positions and relative intensities of different peaks in DOS and $\sigma(\omega)$ may differ from the density function theory predictions (due to many-body effects), the general structure described above should qualitatively hold. This way one can directly verify by spectroscopical means (comparing optical, photoemission and inverse photoemission spectra) the concept of molecular orbitals.

III. DFT CALCULATIONS OF $\sigma(\omega)$ IN $SrRu_2O_6$

We used the full-potential linearized augmented plane-wave (LAPW) method as implemented in the WIEN2k code [20] to calculate optical properties of $SrRu_2O_6$. We used the exchange-correlation potential of Ref. [21]. The spin-orbit coupling has been found to be unimportant in $SrRu_2O_6$ [8, 22], so that we have not included this interaction to the calculations. Similarly, we have found before that the including correlation effects within the dynamical mean-field theory (with modest $U \sim 1$ eV), while renormalizes hopping integrals, leave the entire picture of MOs intact, so in the following we have been using straight DFT. Integration was performed using the tetrahedron method on a mesh consisting of 4096 k-points in the Brillouin zone (BZ). The radii of atomic spheres were

chosen to be 2.36, 1.93 and 1.72 a.u. for Sr, Ru, and O, respectively. The parameter of the plane wave expansion was set to $R_{MT}K_{max}=7$, where R_{MT} is the radius of O and K_{max} is the plane wave cut-off.

For a dielectric, the imaginary part of the dielectric function in the random-phase approximation (RPA) is defined as

$$\text{Im } \varepsilon_{\alpha\beta}(\omega) = \frac{e^2}{\pi m^2 \omega^2} \sum_{c,v} \int \langle c, \mathbf{k}|p^\alpha|v, \mathbf{k}\rangle \langle v, \mathbf{k}|p^\beta|c, \mathbf{k}\rangle$$
$$\times \delta(\epsilon_c(\mathbf{k}) - \epsilon_v(\mathbf{k}) - \hbar\omega)d\mathbf{k}, \tag{5}$$

where m is the electron mass, $\{\alpha, \beta\} = \{x, y, z\}$, summation runs over all pairs of conduction (c) and valence (v) bands, and $\epsilon(\mathbf{k})$ gives the energy of corresponding band, while $\langle c, \mathbf{k}|p^\alpha|v, \mathbf{k}\rangle$ is the momentum operator's matrix element [23]. The real part of the optical conductivity is

$$\text{Re } \sigma_{\alpha\beta}(\omega) = \frac{\omega}{4\pi}\text{Im } \varepsilon_{\alpha\beta}(\omega).$$

This, obviously, includes the phase space factor, usually called the joint density of states,

$$J(\omega) = \sum_{c,v} \int \delta(\epsilon_c(\mathbf{k}) - \epsilon_v(\mathbf{k}) - \hbar\omega)d\mathbf{k},$$

and the effects of the matrix elements. The $J(\omega)$ obtained within the AFM GGA calculations is shown in Fig. 3(a). One observes a broad maximum in the joint DOS at 1.0–1.5 eV, due to the transitions between the E_{2g} and the $E_{1u} + A_{1g}$ manifolds, and another maximum at 1.6-1.8 eV, due to the $B_{1u} \to E_{1u} + A_{1g}$ transitions.

Since $SrRu_2O_6$ has a trigonal crystal structure there are only two independent components in the dielectric tensor, ε_{xx} and ε_{zz}. Fig. 3(c), (d) shows the calculated imaginary part of dielectric tensor components for $SrRu_2O_6$. The amplitude of the ε_{xx} component is about 8 times larger than the one of ε_{zz}, reflecting the fact that it only appears through deviations from the MO model. More interestingly, we observe that $\text{Im }\varepsilon_{xx}(\omega)$ has one strong peak "A" at ~ 1 eV, corresponding to $E_{2g} \to E_{1u}$ transitions, while the second peak of $J(\omega)$ is completely suppressed in $\text{Im }\varepsilon_{xx}(\omega)$ (Fig. 3(c)). Moreover, the first peak also becomes sharper, reflecting the fact that, while the E_{1u} and A_{1g} orbitals are strongly mixed, the higher energy part of the corresponding manyfold has somewhat more of the A_{1g} character, leaving less room for the $E_{2g} \to E_{1u}$ transitions (remember that the $E_{2g} \to A_{1g}$ transitions are forbidden by parity). This is exactly the qualitative effect we were looking for.

Note that if the matrix elements in Eq. (5) are set to a constant, $\langle c, \mathbf{k}|p^\alpha|v, \mathbf{k}\rangle = const$, then $\omega\sigma(\omega) = const \cdot J(\omega)$, and, indeed often in computational papers joint DOS is compared to $\omega\sigma(\omega)$. However, in real materials, $|\langle c|\mathbf{p}|v\rangle|^2/m$ usually grows with energy, roughly as $(E_c - E_v)$ [24], so one can elucidate the suppression of particular transitions by comparing $J(\omega)$ (Fig. 3(a)) with $\sigma(\omega)$ (Fig. 3(b)).

It is worth noting that the structure of $\text{Im}\,\varepsilon_{zz}(\omega)$, which cannot be derived from the MO model, is nonetheless quite interesting. Indeed, the p^z matrix element appears to be strongly enhanced in the very low frequency region, from the absorption edge to about 0.7 eV (the feature denoted "C" in Fig. 3(d)). The matrix elements for next feature, "D", are suppressed by a factor of ≈ 1.5 [2.2-2.3 in $\text{Im}\,\varepsilon_{zz}(\omega)/J(\omega)$], and the high-energy region corresponding to the $B_{1u} \to E_{1u} + A_{1g}$ transitions by an additional factor of ≈ 1.8 (feature "E").

Compared to iridates Na_2IrO_3 and Li_2IrO_3, often quoted in the context of MOs, SrRu_2O_6 has a clear advantage in the sense that in iridates the MO picture is contaminated by a strong spin-orbit interaction that makes selection rules not well expressed. Indeed, while DFT calculations for iridates [25] agree well with experimental data, they cannot be interpreted in such a simple way as ours presented above, and cannot provide such a qualitative assessment of the MO picture. Nevertheless for the sake of completeness below we present a simple tight-binding model, which can be used to investigate optical response not only in the case of three t_{2g} electrons as in SrRu_2O_6, but also for any other occupation.

IV. TIGHT-BINDING TREATMENT OF OPTICAL PROPERTIES IN AN IDEAL MO SYSTEM

While there are three t_{2g} orbitals on each Ru site, so that formally the tight-binding (TB) Hamiltonian is 18×18, only one t_{2g} orbital per site contributes to any given MO[11], so the problem is reduced to 6×6. This allows us to map the full t_{2g} problem onto a simple tight-binding model on an ideal hexagon with one s-orbital per site:

$$H = \begin{pmatrix} 0 & t_1' & t_2' & 0 & t_2' & t_1' \\ t_1' & 0 & t_1' & t_2' & 0 & t_2' \\ t_2' & t_1' & 0 & t_1' & t_2' & 0 \\ 0 & t_2' & t_1' & 0 & t_1' & t_2' \\ t_2' & 0 & t_2' & t_1' & 0 & t_1' \\ t_1' & t_2' & 0 & t_2' & t_1' & 0 \end{pmatrix}, \quad (6)$$

where t_1' and t_2' are the nearest and next-nearest neighbor hoppings via oxygen. Diagonalization of this Hamiltonian gives the spectrum described in the Sec. I.

The dielectric function $\text{Im}\,\varepsilon_{\alpha\beta}(\omega)$ in Eq. (5) is determined by matrix elements of momentum operator $\langle c, \mathbf{k}|p^\alpha|v, \mathbf{k}\rangle$, which can be easily calculated using the matrix elements of the momentum operator in the initial TB basis of $s-$orbitals, defined as [26]

$$\mathbf{p}_{ij} = \frac{im}{\hbar} H_{ij}(\mathbf{R}_i - \mathbf{R}_j),$$

where $\mathbf{R}_i$ and $\mathbf{R}_j$ are the positions of corresponding sites in the hexagon.
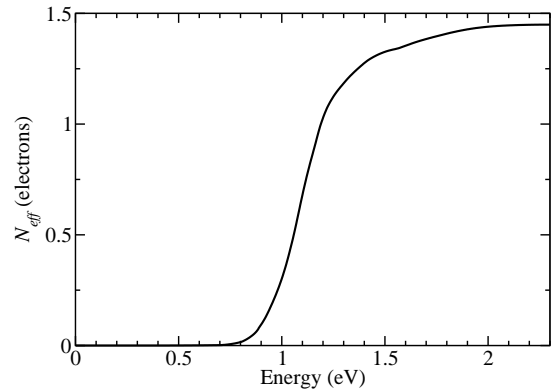

Figure 4: The effective number of electrons obtained for SrRu_2O_6 in the GGA calculation according to Eq. (10) for ε_{xx} component.

The optical transitions can be characterized by their oscillator strengths

$$f_{cv} = \frac{2}{m} \frac{|\langle c, \mathbf{k}|p^\alpha|v, \mathbf{k}\rangle|^2}{E_c - E_v},$$

which can be calculated in the basis of the MOs using eigenvectors of Eq. (6) as a transformation matrix. In our model there are only three nonzero momentum operator matrix elements

$$f_{B_{1u},E_{2g}} = \frac{ma^2}{2\hbar^2}(t_1' - 3t_2'), \quad (7)$$

$$f_{E_{2g},E_{1u}} = \frac{ma^2}{\hbar^2}t_1', \quad (8)$$

$$f_{E_{1u},A_{1g}} = \frac{ma^2}{2\hbar^2}(t_1' + 3t_2'), \quad (9)$$

where a is the distance between the nearest neighbors (3.0053 Å in SrRu_2O_6). This is in agreement with symmetry consideration presented above and results to a single optical $E_{2g} \to E_{1u}$ transition in SrRu_2O_6.

For other fillings, e.g., four or two electrons per transition metal site, one may expect two other transitions, which can be, however, suppressed not due to the symmetry or parity reasons, but because of a particular ratio between hopping parameters. E.g., in both RuCl_3 and SrRu_2O_6, as well as in Na_2IrO_3, the hopping t_2' was found to be of order of $-t_1'/3$ [11, 27], which will result in a strong suppression of the $E_{1u} \to A_{1g}$ transition. If one chose $t_1' = 0.3$ eV and $t_2' = -0.1$ eV as it was estimated for SrRu_2O_6 by Wang et al. [27], then indeed $f_{E_{1u},A_{1g}} \sim 0$, while $f_{B_{1u},E_{2g}} = f_{E_{2g},E_{1u}} = 0.356$.

This provides us with an interesting quantitative check of the validity of the MO model as regards to the full all-electron DFT calculations. A major integral characteristic of the optical absorption is given by the optical sum rule, conveniently written in terms of the effective

number of electrons:

$$\int\limits_{o}^{\omega} Im\ \varepsilon_{\alpha\alpha}(\omega\prime)\omega\prime d\omega\prime = \frac{2\pi^2 e^2}{m\Omega} N_{eff}(\omega), \qquad (10)$$

where Ω is the unit cell volume.

The N_{eff} obtained within *ab initio* calculation from xx component of the dielectric function for $SrRu_2O_6$ is shown in Fig. 4. A plateau in $N_{eff}(\omega)$ curve clearly points to a presence of a single transition in agreement with model and symmetry considerations. For the energy of 2 eV N_{eff}^{xx}=1.44 [28]. In the MO model there is one allowed transition, $E_{2g} \rightarrow E_{1u}$, $f = 0.356$ (using the parameters presented above), and, accounting for symmetry and spin degeneracies, $N_{eff}^{model} = 4f = 1.424$, in excellent agreement with the DFT calculations.

V.   CONCLUSIONS

We presented first principle calculations of the optical properties of the putative molecular orbital solid $SrRu_2O_6$, as well as an analytical analysis of the optical absorption in the molecular orbitals model. We have identified a qualitative signature of molecular orbitals in optical properties. There are only four possible transitions allowed by the parity of the wave functions, but one of these parity-respecting optical transitions is suppressed by the point group symmetry, an unusual effect directly related to molecular orbitals. Different distortions of the crystal lattice, spin-orbit coupling, correlation effects etc. may completely suppress formation of molecular orbitals or strongly modify their structure. We emphasize that one may use optical spectroscopy in the way described above as a probe to identify molecular orbitals in other transition metals oxides consisting of honeycomb layers, even though in the moment $SrRu_2O_6$ is the only viable candidate for a honeycomb MO driven material.

One may also expect that formation of molecular-orbitals in $SrRu_2O_6$ may result in unusual spin excitation spectra. Thus, inelastic neutron scattering may provide another, albeit more indirect way to find signatures of the molecular orbitals.

[1] K. W. Plumb, J. P. Clancy, L. J. Sandilands, V. V. Shankar, Y. F. Hu, K. S. Burch, H.-Y. Kee, and Y.-J. Kim, Phys. Rev. B **90**, 041112 (2014).

[2] J. A. Sears, M. Songvilay, K. W. Plumb, J. P. Clancy, Y. Qiu, Y. Zhao, D. Parshall, and Y.-J. Kim, Phys. Rev. B **91**, 144420 (2015).

[3] Y. Miura, Y. Yasui, M. Sato, N. Igawa, and K. Kakurai, J. Phys. Soc. Japan **76**, 033705 (2007).

[4] J. C. Wang, J. Terzic, T. F. Qi, F. Ye, S. J. Yuan, S. Aswartham, S. V. Streltsov, D. I. Khomskii, R. K. Kaul, and G. Cao, Phys. Rev. B **90**, 161110 (2014).

[5] S. A. J. Kimber, I. I. Mazin, J. Shen, H. O. Jeschke, S. V Streltsov, D. N. Argyriou, R. Valenti, and D. I. Khomskii, Phys. Rev. B **89**, 081408 (2014).

[6] J. Park, T. Tan, D. T. Adroja, A. Daoud-Aladine, S. Choi, D. Cho, S. Lee, J. Kim, H. Sim, T. Morioka, H. Nojiri, V. V Krishnamurthy, P. Manuel, M. R. Lees, S. V. Streltsov, D. I. Khomskii, and J.-G. Park, Sci. Rep. **6**, 25238 (2016).

[7] C. I. Hiley, M. R. Lees, J. M. Fisher, D. Thompsett, S. Agrestini, R. I. Smith, and R. I. Walton, Angew. Chemie - Int. Ed. **53**, 4423 (2014).

[8] S. Streltsov, I. I. Mazin, and K. Foyevtsova, Phys. Rev. B **92**, 134408 (2015).

[9] B. H. Kim, T. Shirakawa, S. Yunoki, arXiv:1606.06836v2

[10] S.M. Winter, Ying Li, H.O. Jeschke, R. Valenti, Phys. Rev. B **93**, 214431 (2016), and unpublished.

[11] I.I. Mazin, H. O. Jeschke, K. Foyevtsova, R. Valentí, and D. I. Khomskii, Phys. Rev. Lett. **109**, 197201 (2012).

[12] In earlier papers [11, 13] the second and the third orbitals were incorrectly labeled as E_{1g} and E_{2u}; the correct symmetries are E_{2g} and E_{1u}.

[13] K. Foyevtsova, H. O. Jeschke, I. I. Mazin, D. I. Khomskii, and R. Valenti, Phys. Rev. B **88**, 035107 (2013).

[14] S. V. Streltsov and D. I. Khomskii Phys. Rev. B **89**, 161112 (2014).

[15] S. V. Streltsov and D. I. Khomskii, Proc. Natl. Acad. Sci. **113**, 10491 (2016).

[16] Z. V. Pchelkina, A. L. Pitman, A. Moewes, E. Z. Kurmaev, T.-Y. Tan, D. C. Peets, J.-G. Park, and S. V. Streltsov, Phys. Rev. B **91**, 115138 (2015).

[17] W. Tian, C. Svoboda, M. Ochi, M. Matsuda, H. B. Cao, J. G. Cheng, B. C. Sales, D. G. Mandrus, R. Arita, N. Trivedi, and J. Q. Yan, Phys. Rev. B **92**, 100404 (2015).

[18] R. L. Flurry, *Quantum Chemistry: An Introduction* (Prentice-Hall, 1983).

[19] E.B. Wilson, J. C. Decius, P.C. Cross, *Molecular vibrations: The Theory of Infrared and Raman Vibrational Spectra* (Courier Corporation, 1955).

[20] P. Blaha, K. Schwarz, G. K. H. Madsen, D. Kvasnicka, and J. Luitz, WIEN2k, An Augmented Plane Wave + Local Orbitals Program for Calculating Crystal Properties

(Techn. Universitat Wien, Wien, 2001).

[21] J.P. Perdew, K. Burke, and M. Ernzerhof, Phys. Rev. Lett. **77**, 3865 (1996).

[22] D. J. Singh, Phys. Rev. B **91**, 214420 (2015).

[23] C. Ambrosch-Draxl and J. O. Sofo, Comput. Phys. Commun. **175**, 1 (2006).

[24] One can understand that from the fact that this relation is exact for the plane waves.

[25] Y. Li, K. Foyevtsova, H. O. Jeschke, and R. Valentí, Phys. Rev. B **91**, 161101(R) (2015).

[26] M. Graf and P. Vogl, Phys. Rev. B **51**, 4940 (1995).

[27] D. Wang, W.-S. Wang, and Q.-H. Wang, Phys. Rev. B **92**, 075112 (2015).

[28] There are three valence electrons in $SrRu_2O_6$, of which this sum rule is missing about 50%; this is mainly due to the missing contribution from the $t_{2g} - e_g$ transitions. It is well known that this geometry induces a large O-assisted nearest-neighbor $t_{2g} - e_g$ hopping (proportional to the product $t_{pd\pi}t_{pd\sigma}$, as opposed to the $t_{pd\pi}^2$, as is the case for $t_{2g} - t_{2g}$ t_1).